THE JOURNAL OF PHYSICAL CHEMISTRY B

ARTICLE

pubs.acs.org/JPCB

Solvent Blends Can Control Cationic Reversed Micellar Interdroplet Interactions. The Effect of *n*-Heptane:Benzene Mixture on BHDC Reversed Micellar Interfacial Properties: Droplet Sizes and Micropolarity

Federico M. Agazzi, R. Dario Falcone, Juana J. Silber, and N. Mariano Correa*

Departamento de Química, Universidad Nacional de Río Cuarto, Agencia Postal # 3, C.P. X5804BYA Río Cuarto, Argentina

Supporting Information

ABSTRACT: We have investigated, for the first time, the effect of the composition of the nonpolar organic media on the benzyl-*n*-hexadecyl-dimethylammonium chloride (BHDC) reversed micelles (RMs) properties at fixed temperature. To achieve this goal we have used the solvatochromic behavior of 1-methyl-8-oxyquinolinium betaine (QB) as absorption probe and dynamic light scattering (DLS), to monitor droplet sizes, interfacial micropolarity, and sequestrated water structure of water/BHDC/*n*-heptane:benzene RMs. DLS results confirm the formation of the water/BHDC/*n*-heptane:benzene RMs at every *n*-heptane mole fraction (X_{Hp}) investigated, that is, X_{Hp} = 0.00, 0.13, 0.21, 0.30, and 0.38. Also, DLS was used to measure the RMs diffusion coefficient and to calculate the apparent droplet hydrodynamic diameter (d_{App}) at different compositions of the nonpolar organic medium. The data suggest that as the *n*-heptane content increases, the interdroplet attractive interactions also increase with the consequent increment in the droplet size. Moreover, the interdroplet attractive interactions can be "switched on (increased)" or "switched off (decreased)" by formulation of appropriate *n*-heptane:benzene mixtures. Additionally, QB spectroscopy was used to obtain the "operational" critical micellar concentration (cmc) and to investigate both the RMs interfacial micropolarity and the sequestrated water structure in every RMs studied. The results show that BHDC RMs are formed at lower surfactant concentration when *n*-heptane or water content increases. When the interdroplet interaction "switches on", the RMs droplet sizes growth expelling benzene molecules from the RMs interface, favoring the water-BHDC interaction at the interface with the consequent increases in the interfacial micropolarity. Therefore, changing the solvent blend is possible to affect dramatically the interfacial micropolarity, the droplet sizes and the structure of the entrapped water.

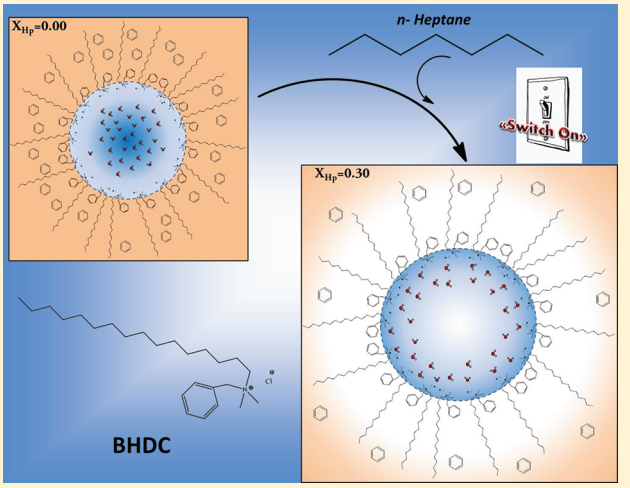

INTRODUCTION

Reversed micelles (RMs), a spatially ordered macromolecular assembly of surfactant molecules randomly distributed in nonpolar media, are of considerable practical importance in detergency, foodstuffs, cosmetics, chemical and biological reactions, separation technology and materials synthesis.[1,2] When surfactants assemble in RMs, their polar or charged groups are located in the interior (core) of the aggregates, while their hydrocarbon tails extend into the bulk organic solvent.[3−5]

Anionic, cationic and nonionic surfactants have been employed to prepare RMs and water-in-oil (W/O) microemulsions in nonpolar solvents.[1−18]Among the anionic surfactants that form RMs, the best known are the systems derived from the AOT (sodium 1,4-bis-2-ethylhexylsulfosuccinate) in different nonpolar media. The cationic surfactant, benzyl-*n*-hexadecyl dimethylammonium chloride (BHDC), also forms spherical RMs in benzene without addition of a cosurfactant and water can be solubilized up to W_0 = [water]/[surfactant] ≈ 25.[8,9,11,13,15,16,18]

It is known that the properties of RMs depend on the type of surfactant and the W_0 values,[1−4,19−21] but the influence of the nonpolar organic pseudophase has scarcely been examined for AOT[12,13,22−25] and, to the best of our knowledge, there are no reports for the BHDC RMs. Probably, the main reason is because BHDC only forms RMs in aromatic solvents, and it is nonsoluble in aliphatic hydrocarbon solvents.

With regard to the interfacial properties changing the surfactant, the BHDC RMs seems to have properties that are characteristic of other reversed micellar systems. This is brought out by the nature

Received: March 31, 2011
Revised: August 18, 2011
Published: September 14, 2011

of the water pool in the BHDC RMs, which show properties similar to that of the bulk water only when the amount of water is higher than the necessary to achieve the surfactant polar head and the counterion solvation.[8,13,18]

Previous studies performed in our group have shown very peculiar and interesting water properties inside RMs that exists only due to the confinement effect and the interaction with the surfactant at the interface. Thus, the water properties are different for water molecules sequestrated inside anionic and cationic RM system. The water molecules entrapped inside the AOT/benzene RM show its electron donor ability enhanced in comparison with its water bulk structure. On the other hand, the water entrapped inside the BHDC/benzene RMs, appear to be non electron donating because its interaction with the cationic surfactant polar headgroup.[19,21]

With regard to the nonpolar organic solvent the most extensive comparative study has been performed for water/AOT/hydrocarbon and water/AOT/benzene RMs. In particular, the thermodynamics of micellization shows that the clustering of benzene molecules around the AOT headgroups appears to be more ordered than is the case for saturated alkanes.[12,26] That is, there is more oil penetration into the AOT RMs interface for the benzene molecules. It turns out that, at the same value of W_0, the aggregation number of AOT is 5 times greater in *n*-hexane than in benzene.[27] Also, ^{1}H NMR studies show that free water can be detected in AOT-benzene RMs, even at low W_0 values.[28] All these studies give evidence of a specific interaction between the AOT polar headgroups and the aromatic solvent decreasing the RMs droplet sizes.

Despite the vast amount of work dealing with microemulsion properties, the question of the microscopic origin of the attractive forces between droplets is still open. As it was discussed, it is well-known that RMs are thermodynamically stable systems over appreciable ranges of composition and temperature.[1,3−5,29] It is generally supposed that AOT RMs behave like hard spheres with a small attractive potential but, the intensity of this potential depends on different parameters, such as temperature, W_0, the presence of electrolyte in the water pool and the nature of the external solvent.[11,29] Thus, a variety of physical phenomena, such as electrical conductivity percolation and phase transition, are observed in these systems upon changing the concentration of the droplets, the temperature and the external nonpolar solvent,[29] having all these phenomena the same origin: the interdroplet interaction. Furthermore, it is not necessary to achieve the phase transition of the systems in order to observe the effect of the interdroplet interaction. For example at a fixed temperature within the reversed micellar stability region of the phase diagram, the interaction is manifested with the increase in the droplet size.[5,11,30−32] Several researchers have shown that the droplet size and the interdroplet interaction can vary changing the composition of the microemulsion.[33] Also, it has been demonstrated that the attraction between droplets depends not only of the size but the fluidity of the interface.[33,34] The question that comes out in these cases is what kind of forces make that two independent droplets attract each other. A possible explanation was given by Lemaire et al.[35] proposing that the attractive interdroplet interactions depend on the mutual interpenetration of the surfactant tails. That is, the surfactant tails between micelles can penetrate each other over some small distance without suffering much entropy loss while lowering the total free energy of the system. This is possible because the surfactant tail−tail interaction is not much stronger than the surfactant−nonpolar external solvent interaction. At finite temperature, the solvent molecules are not optimally oriented to interact with the surfactant tails, while the surfactant tails between two different RMs in the overlap region are always more or less parallel to each other.[35,36] A theory was developed for the calculation of the intermicellar potential resulting from London-van der Waals interatomic attractive interactions.[35] Since the fluctuation of charges in RMs can be considered small, the authors have neglected the possible electrostatic interaction between droplets. A detailed calculation has shown that the most important contribution to the attractive interaction occurred in the overlapping region during the interpenetration of two droplets.[35] Also, the short-range interactions are mainly determined by the overlapping between micelles, which is related to the ability of the continuous phase to penetrate the aliphatic surfactant layer. The overlapping between micelles is accompanied by nonpolar organic solvent removing.[35] Calje et al.[37] have also proposed that these interactions are the result of the difference in the molecular composition between the droplets and the continuous medium.

Recently,[30−32] it was demonstrated that the phase behavior or the properties of W/O microemulsions can be affected by the external nonpolar solvent composition. In this way, it has been shown that it was possible to control the stability of the RMs by applying mixtures of "good" and "bad" solvents to create microemulsions. The concept of "good" and "bad" solvents was used for those solvents that "switch off (decreased)" or "switch on (increased)" the attractive interdroplet interactions, respectively. In other words, a "good" solvent decreases the strength of the interactions between droplets, diminishing the droplet−droplet fusion and, reducing the droplet size of the RMs, while the opposite stands for the "bad" solvents. Their results show that, at a fixed temperature, in mixtures of *n*-heptane ("bad")/toluene ("good") with increasing toluene content, the droplet diffusion coefficient increases and the calculated apparent hydrodynamic diameter (d_{App}) of the RMs droplets decreases. They suggest that attractive interdroplet interactions are "switched off", as the concentration of "good" solvent increases. This very interesting result shows the concept of solvent-induced aggregation (flocculation) of RMs employing blended solvent mixtures. This method of control over colloid stability based on selection of appropriate solvents, is economical and potentially of low energy consumption. The approach to induce reversible stability/instability systems could be applied in separation technology to systems of high-value nanoparticles in order to redisperse and reuse active components readily without affecting the colloid functionality.[30−32]

On the other hand, while droplet interaction plays a predominant role in the size control of the RMs, the nature of the RMs interfaces has to be relevant because mass transfer is not possible unless the interface is ruptured in some way.[22] In this sense, there are no studies performed in BHDC RMs in order to investigate the effect that the external nonpolar solvent has on both: the BHDC interdroplet interactions and the BHDC RMs interface properties within the reversed micellar stability region of the phase diagram.

In this work, we have investigated the water/BHDC/*n*-heptane:benzene RMs using dynamic light scattering (DLS) and the solvatochromism of 1-methyl-8-oxyquinolinum betaine (QB) at a fixed temperature. We have studied the surfactant, water and the external organic solvent content to evaluate interesting RMs properties. DLS experiments show that BHDC RMs are formed in every *n*-heptane:benzene mixture investigated

and, for a given W_0 value the droplet sizes increases as the *n*-heptane content increases. QB, a molecular probe that resides at the RMs interface shows that the micropolarity and the water surfactant interaction change dramatically with the nonpolar organic solvent composition. We have discussed the results taken into consideration how the solvent penetration to the interface affects the interdroplet interaction and the water−surfactant interaction.

EXPERIMENTAL SECTION

Materials. Benzene (Bz) and *n*-heptane (Hp) all from Merck, HPLC grade, were used without further purification.

Benzyl-*n*-hexadecyl-dimethylammonium chloride (BHDC) from Sigma (>99% purity) was recrystallized twice from ethyl acetate.[13] BHDC was dried under reduced pressure, over P_2O_5 until constant weight. 1-Methyl-8-oxyquinolinium betaine (QB) was synthesized by a procedure reported previously.[38] The UV−vis spectra of QB in the presence of BHDC RMs showed that the surfactant is free of acidic impurities, which would have greatly reduced the intensity of the solvatochromic B_1 band at 502 nm.[12,13]

Ultrapure water was obtained from Labonco equipment model 90901−01.

Methods. The *n*-heptane: benzene solutions at any *n*-heptane bulk mole fraction, X_{Hp} values, composition studied were prepared by weight.

The stock solutions of BHDC in *n*-heptane:benzene mixture were prepared by weight and volumetric dilution. To obtain optically clear solutions they were shaken in a sonicating bath and, water was added using a calibrated microsyringe. The amount of water present in the system is expressed as the molar ratio between water and the surfactant ($W_0 = [\text{water}]/[\text{BHDC}]$). The lowest value for W_0 ($W_0 = 0$), corresponds to a system without the addition of water.

To introduce the molecular probe, a 0.01 M solution of QB was prepared in methanol (Sintorgan HPLC quality). The appropriate amount of this solution to obtain a given concentration (2×10^{-4} M) of the probe in the micellar medium was transferred into a volumetric flask, and the methanol was evaporated by bubbling dry N_2; then, the BHDC RMs solution was added to the residue to obtain a [BHDC] = 0.2 M in any X_{Hp} mixture investigated. The stock solution of surfactant 0.2 M and the molecular probe were agitated in a sonicating bath until the microemulsion was optically clear. To the cell baring 2 mL of QB of the same concentration in the different *n*-heptane:benzene mixtures, was added the appropriate amount of surfactant and molecular probe stock solution to obtain a given concentration of surfactant in the micellar media. Therefore, the absorption of the molecular probe was not affected by dilution.

General. UV−vis spectra were recorded using a spectrophotometer Shimadzu 2401 with a thermostatted sample holder. The path length used in absorption experiments was 1 cm. All experimental points were measured three times with different prepared samples. The pooled standard deviation was less than 5%. All the experiments were carried out at 32.0 ± 0.5 °C.

The apparent hydrodynamic diameters of the different BHDC RMs were determined by dynamic light scattering (DLS, Malvern 4700 with goniometer) with an argon-ion laser operating at 488 nm. BHDC RMs samples were filtered using an Acrodisc with 0.2 μm PTFE membrane (Sigma). Viscosities and refractive indices of the solvent mixtures are required for the DLS analyses: the viscosities of *n*-heptane:benzene systems were taken from the literature.[39] The refractive indices of the solvent mixtures were calculated using a first-order approximation (eq 1)

$$\eta_D = X_1\eta_{D1} + X_2\eta_{D2} \quad (1)$$

where η_{D1} and η_{D2} are the pure solvent refractive indices. The effect of temperature on η_D of these solvents was found to be sufficiently small to be ignored[30] Multiple samples for each size were made, and thirty independent size measurements were made for each individual sample at the scattering angle of 90°. The algorithm used was CONTIN, the apparent hydrodynamic diameters values reported were weighted by intensity, volume and/or number since no differences are observed. The DLS experiments show that the polidispersity of the BHDC RMs size is less than 5%.

RESULTS AND DISCUSSION

QB in *n*-Heptane:Benzene Homogeneous Mixtures. The QB absorption spectra in the *n*-heptane:benzene binary mixture at different X_{Hp} are shown in Figure S1, in the Supporting Information section. As it can be seen, QB presents two electronic absorption bands B_1 and B_2, which sense different effects as we have previously demonstrated[12,13] The band in the visible region, B_1, is due to the transition from a predominantly dipolar ground state to an excited state of considerably reduced polarity. It was found that the B_1 solvatochromism is mainly due to the polarity/polarizability ability of the medium. However, this band also correlates with the H-bond donor ability of the medium.[12] With increasing the polarity or the H-bond donor ability of the solvent, the ground state becomes more stable, which leads to an increase in the transition energy, that is, negative solvatochromism. The transition energy (expressed in kcal mol^{-1}) of QB can be used as a polarity parameter, E_{QB}, similar to the Dimroth et al. $E_T(30)$ value[40] because it has been shown that E_{QB} value correlates in a linear relationship with this solvent parameters through eq 2.[38]

$$E_T(30) = 1.71E_{QB} - 49.1 \quad (2)$$

The band in the UV region, B_2, which was assigned to a charge transfer from the phenoxide ion to the aromatic ring (Scheme 1), also shifts hypsochromically with the polarity of the solvent, although in lesser magnitude than the visible band.[12] Moreover, it was shown that the B_2 band frequency is also sensitive to the H-bond donor capability of the solvent.[12] Interestingly, the absorbance ratio of both bands ($Abs B_2/Abs B_1$) is quite sensitive to the H-bond ability of the medium.[12] $Abs B_2/Abs B_1$ value is large for solvents with low H-bond ability and decreases as the solvent H-bond capability increases. Consequently, the $Abs B_2/Abs B_1$ ratio is used in combination with the absorption bands shifts to determine the properties of the microenvironment surrounding the probe.[12,13] Nevertheless, recent results[41] suggest that other factors should be also responsible for the QB ratio absorbances values as we will discuss later.

Figure 1 A shows the plot of the $E_T(30)$ parameter values obtained through eq 2[38] for the *n*-heptane:benzene binary mixture as a function of the heptane bulk mole fraction, X_{Hp}. As it can be observed the experimental points does not deviate from linearity in the whole X_{Hp} range studied and, also shows decreases of the $E_T(30)$ values with the increasing proportion of *n*-heptane as result of the decreasing of the polarity of the medium.[42,43] This result is rather interesting because QB is not

Scheme 1. Molecular Structure of the Molecular Probe Used: QB and the BHDC Surfactant

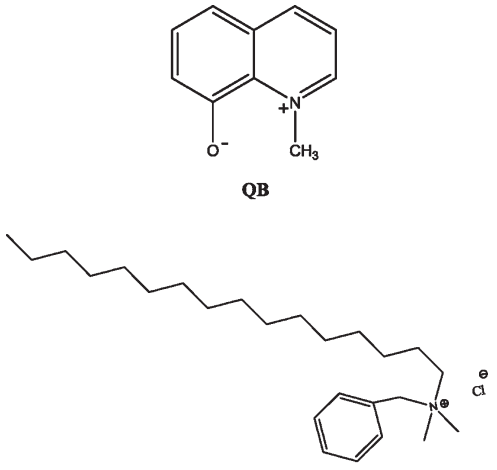

soluble in *n*-heptane but, it seems that it can be solvated by the *n*-heptane:benzene mixture which behaves as a "regular" solution.[44] Very recently[43] we have found that QB is solvated preferentially by glycerol in a dimethylformamide-glycerol mixture result that demonstrates the importance of the hydrogen bond interaction on the QB solvatochromism.

Figure 1 B shows the plot of the Abs B_2/Abs B_1 ratio values as a function of X_{Hp}. As it can be seen, there is no variation on the ratio values which means that there is no specific interaction between QB and the surroundings.

Study in BHDC/n-Heptane:Benzene Reversed Micelles. Figure 2 shows the maximum amount of water (W_{0Max}) as a function of X_{Hp} that the BHDC RMs systems can accept showing a transparent and stable single phase. That is, in the RMs stability region (single clear phase) of the phase diagram where there is no phase transition separation. Above this threshold the media becomes cloudy when the phase transition occurs. It is clear that the W_{0Max} values decrease as the *n*-heptane content increases and, the amount of water decreases dramatically at X_{Hp} above 0.13. It must be noted that BHDC is a surfactant that cannot be dissolved and does not form RMs in saturated hydrocarbons. Consequently, X_{Hp} = 0.59 is the maximum amount of *n*-heptane that can be added to the system producing optically clear solution. After that, the system collapses (phase transition). Therefore, benzene plays a major role in the RM stabilization. In this way, for BHDC the aromatic solvent is a "good" solvent in the sense that RMs can be formed and are stable. On the other hand and following this argument we define *n*-heptane as a "bad" solvent for BHDC since the surfactant solubility is negligible and the presence of RMs cannot be detected. Similar definitions were introduced by other authors in water/AOT/toluene:/*n*-heptane RMs.[30,31] However, the main difference between AOT and BHDC is that the anionic surfactant can form RMs in both solvents.

A question may arise here that if the water is effectively encapsulated by the surfactant creating a true RMs media in every solvent mixture investigated. DLS is used to assess this matter for water/BHDC in the different *n*-heptane:benzene mixtures, because it is a powerful technique to evaluate the formation of RMs.[3−5,45−49] Thus, if water is really encapsulated to form RMs, the droplets size must increase as the W_0 value increases with a

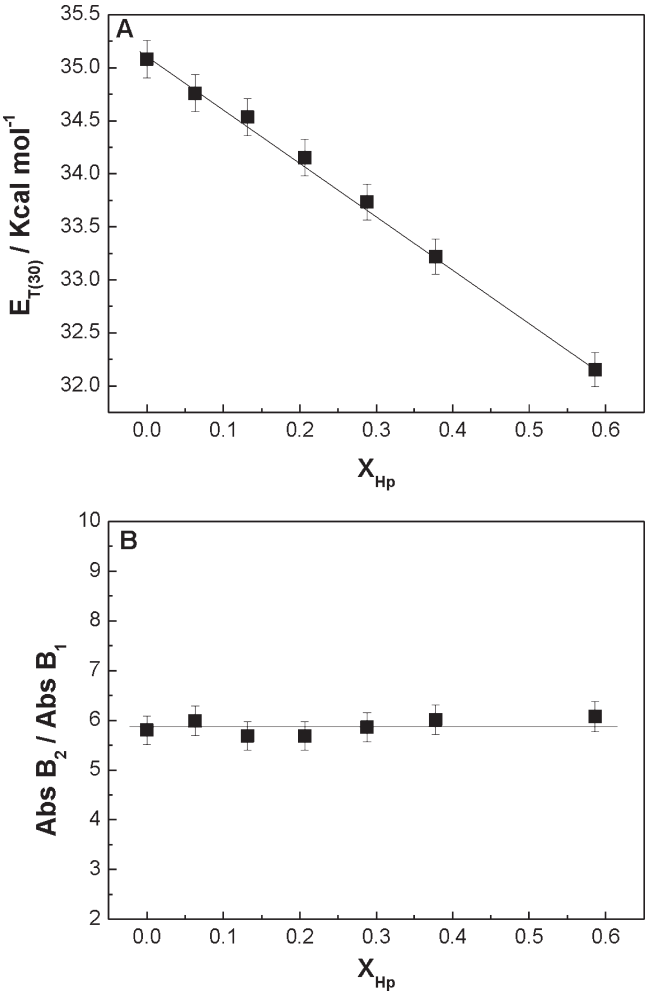

Figure 1. Variation of (A) $E_T(30)$ values and (B) AbsB_2/AbsB_1 ratio values, as a function of X_{Hp} for *n*-heptane:benzene mixture. [QB] = 2 × 10^{-4} M. The straight line was plotted to guide the eye; it represents no preferential solvation of QB by the mixture.

linear tendency (swelling law of RMs) as it is well established for water or polar solvents/surfactant RMs systems.[3,45,46] This feature can also demonstrate that the water/BHDC/*n*-heptane: benzene RMs media consist of discrete spherical droplets.[47]

In our work, all the DLS experiments were carried out at fixed BHDC concentration of 0.1 M. Thus, the RMs solutions are not at infinite dilution, nevertheless we think appropriate to introduce an apparent hydrodynamic diameter (d_{App}) to make the comparison of our systems. A similar approach was used by other authors.[30] In Figure 3 we report the d_{App} values obtained in water/BHDC/*n*-heptane:benzene systems for X_{Hp} = 0 and 0.13 (A) and X_{Hp} = 0.30 and 0.38 (B) at [BHDC] = 0.1 M. As can be seen the *n*-heptane molar fractions shown in Figure 3 A correspond to the systems that accept large amount of water (rich in "good" solvent) while the ones shown in Figure 3 B correspond to the systems where the W_{0Max} values decrease dramatically as shown in Figure 2 (rich in "bad" solvent). In all the systems studied it can be observed that there is an increase in d_{App} when the W_0 value increases. The linear tendency observed in Figure 3 shows that water is effectively sequestrated by BHDC yielding RMs in every solvent mixture studied which consist on discrete spherical droplets.

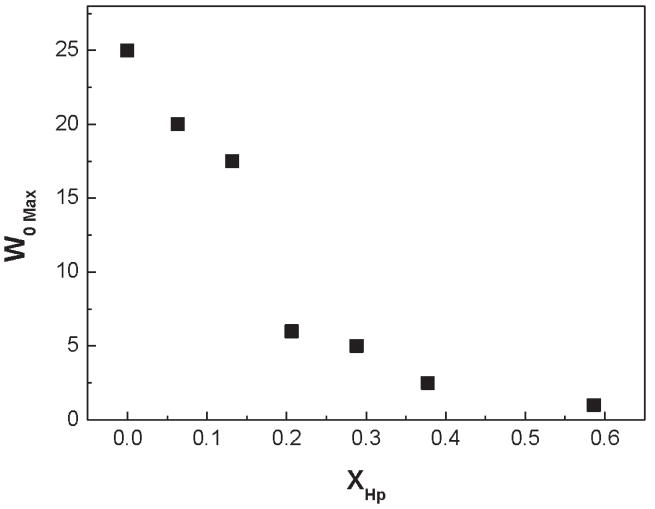

Figure 2. W_{0Max} values as a function of X_{Hp} for water/BHDC/*n*-heptane:benzene reversed micelles media. [BHDC] = 0.1 M.

The water/BHDC/*n*-heptane: benzene RM droplet sizes shown in Figure 3 A are significantly lower than the droplet sizes shown in Figure 3 B. For example at $W_0 = 2$, the droplet size for the RMs at $X_{Hp} = 0$ is 3.0 nm, while for $X_{Hp} = 0.38$ is 5.2 nm. Thus, as the nonpolar phase become richer in *n*-heptane, the droplet size of the RMs increases, at any W_0 value studied. Salabat et al.[30] have shown the effect of solvents on stability of water/AOT/*n*-heptane:toluene RMs at different *n*-heptane and solvent mixtures using DLS. They have shown that at fixed temperature in the mixtures of *n*-heptane/toluene with increasing the toluene mole fraction, the droplet diffusion coefficient increases and the calculated apparent hydrodynamic diameter of RMs droplets decreases. They suggested that interdroplet attractive interactions are "switched off", and that interdroplet interactions decrease in magnitude as the toluene concentration increases. It is known[30,50] that the dynamics process (kinetic effect) of droplet collisions (continually occurring as fusion-splitting of droplets in equilibrium RMs) occurs over a millisecond-microsecond time scale for AOT/*n*-heptane RMs. Hence, adding the "bad" solvent aggregation of droplets is extremely rapid, followed by a much slower gravitational settling, and resulting in an eventual phase resolution of the coarse emulsion droplets. Moreover, from a thermodynamic point of view, even far from the phase transition separation the interdroplet interaction may result in a bigger and stable RMs droplet. On the other hand, increasing the toluene mole fraction ("good" solvent) at a fixed temperature within the stability region of the phase diagram, the apparent diffusion coefficient increases. Thus, they showed that the attractive interactions between particles decreases, increasing the mole fraction of toluene.[30] Lemaire et al.,[35] Calje et al.,[37] and Brunetti et al.[51] have shown that the magnitude of interdroplet attractive interactions increase with the difference between the composition of the interface and the continuous nonpolar phase. The increasing difficulty in penetrating the interface by larger oil molecules would increase this difference, thus increasing the magnitude of the interaction. Thus, decreasing the oil chain length also decreases the net interdroplet attraction. The larger radius of gyration of the longer chains prevents them from close packing on the surfactant interface. The surfactants from other droplets are optimally packed and hence have a larger net attraction.

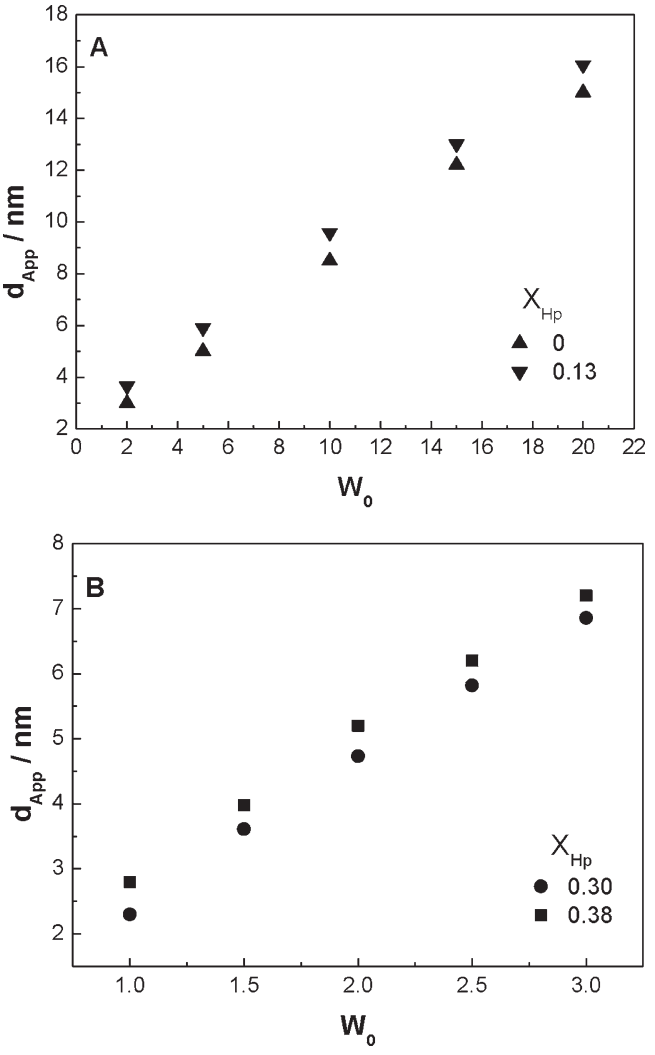

Figure 3. Water/BHDC/*n*-heptane:benzene droplets apparent diameters (d_{App}) as a function of W_0 for (A) $X_{Hp} = 0.00$ (▲) and 0.13 (▼); (B) $X_{Hp} = 0.30$ (●) and 0.38 (■). [BHDC] = 0.1 M.

As the oil chain length decreases, the difference between oil and surfactant packing decreases and the net attraction of two droplets is thus reduced.[52]

The results reported in Figure 3 show that the same analysis can be extrapolated to the BHDC RMs where, as the *n*-heptane content increases the interdroplet attractive interactions increase with the consequent increment in the droplet size. In this sense we notice that, although the origin of attractive forces in RMs is still not clear,[29] the oil penetration to the interface are thought to be a major factor; in fact the lesser the oil penetration to the interface, the greater is the difference in composition between the interface and the nonpolar phase and the greater is the interdroplet interaction giving a bigger and thermodynamically stable BHDC RMs. For AOT, it is known that as the molar volume (V_M) of the oil diminishes, the penetration into the interface is favored and the difference in composition between the RM interface and the oil phase is diminished. Consequently, the interdroplet attractive interaction diminishes in magnitude and the droplet size decreases. Moreover, the RMs curvature C_o depends both on the composition of the phases it separates and on surfactant type. One argument applied to the nonpolar side of

the interface is that nonpolar organic solvent can penetrate to some extent between the surfactant hydrocarbon tails. The more extensive the penetration, the more curvature is imposed toward the polar side. This results in a decrease of C_o (and RMs droplet size) since, by convention, positive curvature is toward oil (and negative toward water). The longer the oil chains, the less they penetrate the surfactant film and the smaller the effect on C_o. The effect of alkane structure, and molecular volume on the nonpolar organic solvent penetration was also investigated with *n*-heptane, and cyclohexane. The results indicate that *n*-heptane is essentially absent from the interface, but the more compact cyclohexane has a greater penetrating effect.[53] Thus, for AOT RMs the rigid benzene molecule (V_M = 89.8 cm^3 mol^{-1}) penetrates easily to the RMs interface in comparison to *n*-heptane (V_M = 146.5 cm^3 mol^{-1}), being AOT/benzene RMs smaller than the AOT/*n*-heptane RMs at the same W_0 value.[12,13,22] This is one of the reasons that makes the AOT/benzene RMs smaller than the AOT/*n*-heptane RMs. It must be taken into account that because the nonpolar organic solvents thermal energy, they are always in a random movement that prevent them to reach the RMs interface in a particular order. Thus, the larger radius of gyration of *n*-heptane in comparison with benzene prevents it from close packing on the surfactant interface increasing the magnitude of the interdroplet attractive interactions.

On the other hand, it is known[54] that the RMs droplet sizes depend, among many other variables, on the effective packing parameter of the surfactants, v/al_c, in which v and l_c are the volume and the length of the hydrocarbon chain, respectively and a is the surfactant headgroup area. The RMs sizes are larger when the surfactant packing parameter values are smaller.[55,56] Thus, all the factors that make decreases the v values or increases a values would make the packing parameter to decrease. Our DLS results suggest that, in BHDC RMs as the *n*-heptane mole fraction increases, the interdroplet interaction also increases making the RM droplets size larger. Therefore, as the *n*-heptane content increases the overlapping between droplets is probably accompanied by benzene removing from the interface.[35] Thus, the v and the surfactant packing parameter values decrease, with the consequent increases in the droplet size.

On the other hand, when water is encapsulated in AOT/isooctane RMs, the H-bond interaction with the AOT polar headgroup increases the surfactants' a values with the consequent decrease in the surfactant packing parameter and, the increase in the RM droplet size. Maitra demonstrated that the AOT's a value increases from 36 to 51 $Å^2$ as the W_0 value increases from 4 to 20 because the water molecules bind to the AOT polar headgroup at the RM inteface.[54] Also, we have recently[57] shown using DLS that, besides water, in non aqueous AOT/*n*-heptane RMs the polar solvents-AOT interactions, especially the hydrogen bond, are the key for the RMs droplets sizes control. In summary, water (or polar solvent)−surfactant interaction increases the effective interfacial area, decreasing the surfactant packing parameter and increasing the RMs size. Thus, it seems that as the *n*-heptane content increases the water−BHDC interaction should be favored in order to make larger the effective interfacial area value with the consequent decreases of the surfactant packing parameter.

In summary, our DLS data suggest that as the *n*-heptane content increases the surfactant packing parameters should decrease probably making that (i) benzene molecules expel from the RMs interface decreasing the effective interfacial volume and (ii) the BHDC interface is more rich in interfacial water molecules favoring the BHDC−water interaction and increasing the effective interfacial area.

As expected, not only the interdroplet interaction but the RMs interfacial properties and the water−surfactant interaction changes as the nonpolar phase composition is altered. To investigate this effect, we use the absorption spectroscopy of QB since B_1 and B_2 bands are sensitive to different effects as it was previously discussed.

Studies Using QB As Molecular Probe. It is important to note that despite that QB is soluble in benzene and can experience a partition process between two different pseudophases: the RMs and the organic solvent, we have previously shown in water/BHDC/benzene[13] and 1-butyl-3-methylimidazolium tetrafluoroborate or 1-butyl-3-methylimidazolium bis(trifluoromethylsulfonyl)imide/BHDC/benzene RMs[41] at any polar solvent content, that the molecular probe resides mainly at the RMs interface because of a strong interaction between the cationic polar head of the surfactant and the QB aromatic ring.[13] Thus, QB can monitor the changes at the BHDC RMs interfaces, probably at the same level as the surfactant headgroup. It must be noted that QB as any other molecular probe, reports only its environment that is necessarily perturbed.

Typical QB spectra in BHDC RMs at X_{Hp} = 0.30 varying the surfactant concentration at W_0 = 0 and 5 are shown in Figure S2 A and B, respectively in the Supporting Information section. Similar spectra are observed in all the RMs investigated (not shown). We have investigated the water addition up to W_0 = 5, in which case the maximum amount of *n*-heptane that yields transparent RMs solution is X_{Hp} = 0.30 (Figure 2). Figures 4 A and B show the λ_{max} B_1 values for QB in water/BHDC/*n*-heptane: benzene RMs varying [BHDC] at different X_{Hp} and at W_0 = 0 and 5, respectively. The plots show an increase in the micropolarity of the medium as the surfactant concentration increases at both W_0 values. Figure 4A shows that the λ_{max} B_1 values show differences with the *n*-heptane content up to [BHDC] = 0.05 M. After that no variation of the micropolarity sensed by QB is observed. On the other hand, Figure 4 B shows that the micropolarity values of the RMs are always higher for the systems with high *n*-heptane content. As the DLS results suggest, the presence of *n*-heptane in the solvent mixtures favors the interdroplet attractive interaction, expelling benzene molecules from the interface and favoring the water−BHDC interaction at the interface. Consequently, as observed in Figure 4 B, QB senses higher RMs micropolarity for X_{Hp} = 0.30 than for the measured at other values of X_{Hp} probably because the BHDC RMs interface is richer in water.

In addition, Figure 4 A and B show that there is a concentration range where the micropolarity changes dramatically and, the operational micellar concentration, cmc, can be obtained for the different RMs. The results obtained for the different systems are gathered in Table 1. Two conclusions are extrapolated from the results: i) The BHDC RMs are formed at lower surfactant concentration for systems with higher *n*-heptane content; that is the cmc values are lower as X_{Hp} increases. This fact can be explained considering that the BHDC solubility decreases as the *n*-heptane content increases; ii) The presence of water favors the RMs formation as it was observed for other reversed micellar media.[1,3,4]

Figure 5 A shows the $AbsB_2/AbsB_1$ ratio values for BHDC RMs at different X_{Hp} at W_0 = 0, and Figure 5 B and C show the ratio values for different X_{Hp} at W_0 = 5. The trends observed for the $AbsB_2/AbsB_1$ ratio in Figures 5 A are unexpected and

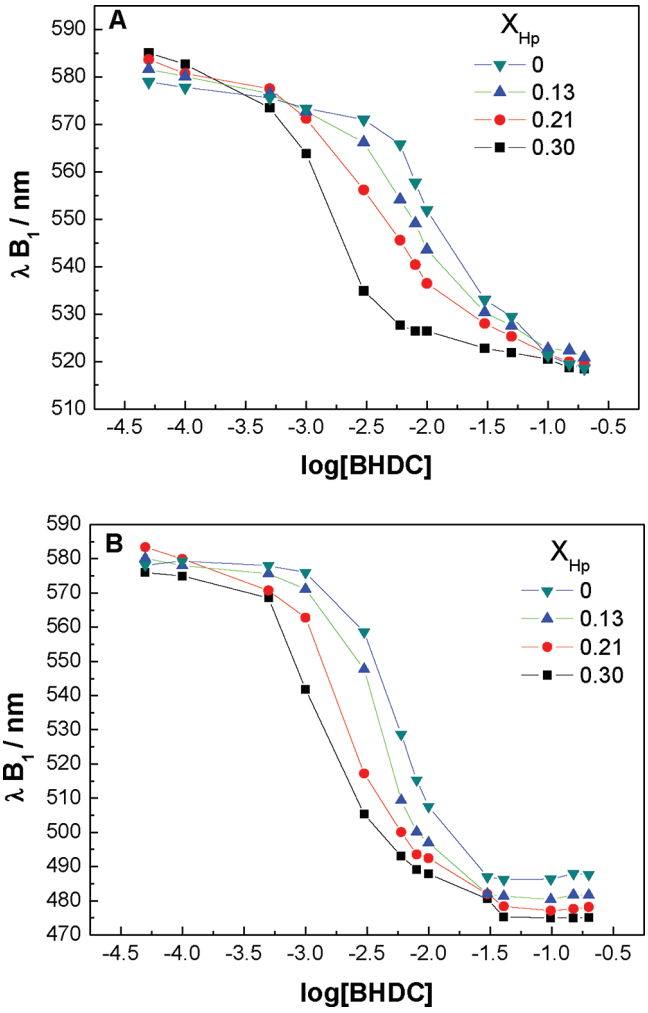

Figure 4. B_1 λ_{max} values as a function of log [BHDC] for water/BHDC/*n*-heptane/benzene reversed micelles media at different X_{Hp} values for: (A) $W_0 = 0$ and (B) $W_0 = 5$. [QB] = 2×10^{-4} M.

Table 1. Critical Micellar Concentration (cmc) for BHDC/*n*-Heptane/Benzene Reversed Micelles Media at Different X_{Hp} and W_0 Obtained by QB Solvatochromism. [QB] = 2×10^{-4} M

X_{Hp}	$W_0 = 0$ (cmc/M)	$W_0 = 5$ (cmc/M)
0.00	$(1.0 \pm 0.2) \times 10^{-2}$	$(6.0 \pm 0.2) \times 10^{-3}$
0.13	$(6.0 \pm 0.2) \times 10^{-3}$	$(4.0 \pm 0.4) \times 10^{-3}$
0.21	$(4.0 \pm 0.6) \times 10^{-3}$	$(2.0 \pm 0.3) \times 10^{-3}$
0.30	$(2.0 \pm 0.1) \times 10^{-3}$	$(1.0 \pm 0.2) \times 10^{-3}$

different from the results shown in Figure 1 B. We were expecting no variation of the ratio since at $W_0 = 0$ there are no possibility of hydrogen bond interaction between QB and the surrounding. Recently, we have discovered certain facts that lead us to think that other factors that have not hitherto been considered should also be responsible for the QB ratio absorbances values changes beside the H-bond donor ability of the microenvironment. For example, we have observed[41] that the $AbsB_2/AbsB_1$ values of QB found in neat ionic liquids (ILs) are surprisingly high. We have suggested an extra interaction (electrostatic) between QB and

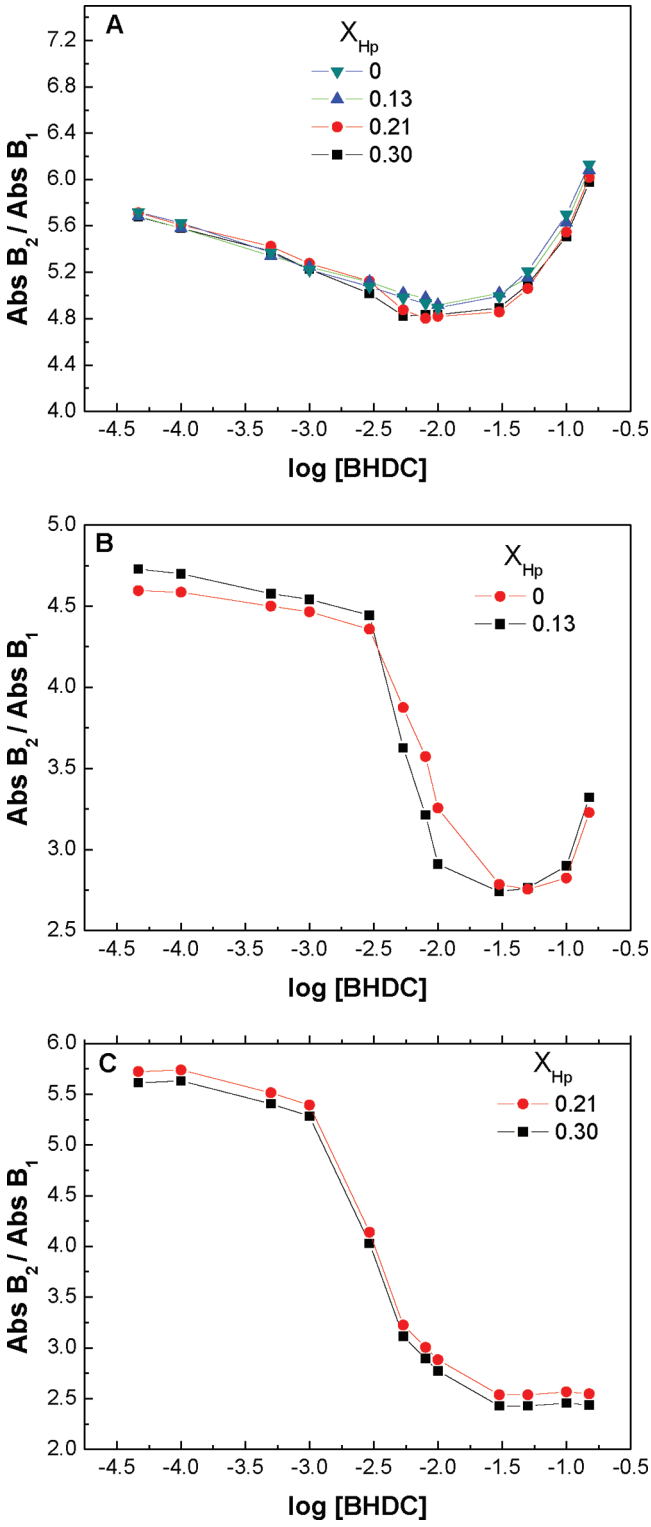

Figure 5. Abs B_2/Abs B_1 ratio values as a function of log [BHDC] for water/BHDC/*n*-heptane:benzene reversed micelles media at different X_{Hp} values for: (A) $W_0 = 0$; (B) $W_0 = 5$, and (C) $W_0 = 5$. [QB] = 2×10^{-4} M.

the ILs ions other than the expected H-bond interaction, to explain the anomalous results. The unexpected absorbance ratio values observed in neat ILs could be a consequence of competitive interactions between cations−QB or anions−QB, that decreases the B_1 absorption band intensity increasing the

absorbance ratio value obtained. QB (Scheme 1), bears a negative charge (the phenolate oxygen) and positive charge (the pyridinium ring) suitable for electrostatic interaction with cations and anions respectively. Thus, the Abs B_2/Abs B_1 ratio values obtained in the ILs studied were explained considering the effect that the ion pair effect has on the QB−ILs interaction.

Herein, the QB spectra shown in Supporting Information Figure S2A for BHDC RMs at W_0 = 0, suggest that the main reason of the increases in the Abs B_2/Abs B_1 ratio values (Figure 5 A) is also the diminishing in the B_1 absorbance band. To explain this interesting result we have to invoke the QB-BHDC interaction suggested in previous work.[13] It seems that there is an electrostatic interaction between the positive charge of the BHDC polar headgroup and the negative charge of QB (phenolate ring), which alters the QB intramolecular charge transfer band, diminishing the molar extinction coefficient of the B_1 band. Moreover, the QB−BHDC interaction is a phenomenon that happens at the BHDC RMs interface since the absorbance ratio values change once the micelles are formed, that is, above the cmc value. It must be noted that BHDC is a surfactant that has a benzyl group in its moiety (Scheme 1). It seems that the electrostatic interaction between QB and the positive charge that the polar headgroup holds, dominates QB spectroscopy over the polarizability effect that the benzyl group may provide. Moreover, McNeil et al.[8] demonstrated that the benzyl group is located toward the surfactant chain, and toward the bulk nonpolar phase.

On the other hand, the situation is different when water is added to the RMs and, the results depend on the X_{Hp} values. Figure 5 B shows that at low *n*-heptane content, X_{Hp} = 0 and 0.13, QB senses H-bond interaction (diminishing in the absorbance ratio value) with water until the cmc value, but once the BHDC RMs are formed, QB−BHDC interaction is stronger than QB−water interaction, and the absorbance ratio value increases.

On the other hand, Figure 5 C shows that for X_{Hp}= 0.21 and 0.30 the situation is quite different. Herein, QB−water interaction is the strongest, and the changes in the absorbances ratio values are the expected for a H-bond donor environment. Please noted that, as was explained for W_0 =0, QB spectroscopy is not dominated for the BHDC benzyl group. As it was suggested in the DLS section, as the X_{Hp} increases the RMs droplet sizes are larger and, the benzene molecules are expelled from the interface. In this way, water molecules penetrate the interface to solvate the cationic surfactant through its nonbonding electrons. QB detects a more polar (Figure 4 B) and H-bond donor environment. These singular results suggest that not only the BHDC RMs sizes change upon the "bad" solvent addition (as it was previously shown for AOT RMs),[30] but the BHDC RMs interface and the interfacial water property vary with the nonpolar phase composition. Thus, BHDC RMs formed in pure "good" solvent are the smallest and have an interface rich in benzene. When *n*-heptane is added, the BHDC RMs droplet sizes increase and the interface have more water molecules interacting with the cationic polar head of the surfactant through their nonbonding electrons. Thus, we show that in BHDC reversed micellar media, the interfacial composition depends on the nonpolar phase blend.

CONCLUSIONS

In this paper, we have investigated, for the first time, the solvent blends effect on interfacial properties of the cationic BHDC reversed micellar media. We have shown using QB absorption and DLS technique that, the BHDC droplet sizes, the interfacial micropolarity and the water−BHDC interaction depend dramatically on the nonpolar organic medium composition. Thus, our results suggest that not only the BHDC RMs sizes change upon the *n*-heptane addition (as it was previously shown for AOT RMs),[30] but the BHDC RMs interfacial composition vary with the nonpolar phase blend.

Thus, we have shown that BHDC RMs formed in *n*-heptane ("bad")/benzene ("good") mixtures increases droplet sizes, the interfacial micropolarity, and the water-polar head surfactant interaction as the *n*-heptane content increases.

Finally, our work show how the interdroplet attractive interactions can be "switched on (increased)" or "switched off (decreased)" by formulation of appropriate *n*-heptane:benzene mixtures, with the consequent variation of the cationic reversed micelles interfacial composition. We hope that the results can be employed in nanoparticle synthesis and in separation process.

ASSOCIATED CONTENT

Supporting Information. Figures showing QB absorption spectra in the *n*-heptane: benzene mixture at different X_{Hp} values and QB absorption spectra in water/BHDC/*n*-heptane: benzene reversed micelles media at X_{Hp} = 0.30 at different BHDC concentration, (A) W_0 = 0 and (B) W_0 = 5. This material is available free of charge via the Internet at http://pubs.acs.org.

AUTHOR INFORMATION

Corresponding Author
*E-mail: mcorrea@exa.unrc.edu.ar.

ACKNOWLEDGMENT

We gratefully acknowledge the financial support for this work by the Consejo Nacional de Investigaciones Científicas y Técnicas (CONICET), Agencia Córdoba Ciencia, Agencia Nacional de Promoción Científica y Técnica and Secretaría de Ciencia y Técnica de la Universidad Nacional de Río Cuarto. N. M.C., J.J.S. and R.D.F. hold a research position at CONICET. F. M.A. thanks CONICET for a research fellowship. We also want to thank reviewer 2 for his/her careful and thorough review of this manuscript.

REFERENCES

(1) (a) Moulik, S. P. *Curr. Sci.* **1996**, *71*, 368–376. (b) Moulik, S. P.; Paul, B. K. *Adv. Colloid Interface Sci.* **1998**, *78*, 99–195.
(2) Uskokovic, V.; Drofenik, M. *Adv. Colloid Interface Sci.* **2007**, *133*, 23–34.
(3) Silber, J. J.; Biasutti, M. A.; Abuin, E.; Lissi, E. *Adv. Colloid Interface Sci.* **1999**, *82*, 189–252.
(4) De, T. K.; Maitra, A. *Adv. Colloid Interface Sci.* **1995**, *59*, 95–193.
(5) Moulik, S. P.; Paul, B. K. *Adv. Colloid Interface Sci.* **1998**, *78*, 99–195.
(6) (a) Fendler, J. H. *Acc. Chem. Res.* **1976**, *9*, 153–161. (b) Fendler, J. H. *Membrane Mimetic Chemistry*; Wiley Interscience: New York, 1982; Chapter 3.
(7) (a) Gu, J.; Shelly, Z. A. *Langmuir* **1997**, 4256–4266. (b) Mandal, D.; Datta, A.; Kumar Pal, S.; Bhattacharyya, K. *J. Phys. Chem. B* **1998**, *102*, 9070–9073. (c) Zhu, D. M.; Wu, X.; Schelly, Z. A. *Langmuir* **1992**, *8*, 1538–1540. (d) Zhu, D. M.; Feng, K.; Schelly, Z. A. *J. Phys. Chem.* **1992**, *96*, 2382–2385.
(8) McNeil, R.; Thomas, J. K. *J. Colloid Interface Sci.* **1981**, *83*, 57–65.

(9) Costa, S. M. B; Brookfield, R. L. *J. Chem. Soc., Faraday Trans. 2* **1986**, *82*, 991–1002.
(10) Jada, A.; Lang, J.; Zana, R. *J. Phys. Chem.* **1990**, *94*, 381–387.
(11) Jada, A.; Lang, J.; Zana, R.; Makhloufi, R.; Hirsch, E.; Candau, S. J. *J. Phys. Chem.* **1990**, *94*, 387–395.
(12) Correa, N. M.; Biasutti, M. A.; Silber, J. J. *J. Colloid Interface Sci.* **1995**, *172*, 71–76.
(13) Correa, N. M.; Biasutti, M. A.; Silber, J. J. *J. Colloid Interface Sci.* **1996**, *184*, 570–578.
(14) Correa, N. M.; Levinger, N. E. *J. Phys. Chem. B* **2006**, *110*, 13050–13061.
(15) Novaira, M.; Biasutti, M. A.; Silber, J. J.; Correa, N. M. *J. Phys. Chem. B* **2007**, *111*, 748–759.
(16) Correa, N. M.; Durantini, E. N.; Silber, J. J. *J. Org. Chem.* **2000**, *65*, 6427–6433.
(17) Correa, N. M.; Durantini, E. N.; Silber, J. J. *J. Org. Chem.* **1999**, *64*, 5757–5763.
(18) Grand, D.; Dokutchaev, A. *J. Phys. Chem. B* **1997**, *101*, 3181–3186.
(19) Quintana, S. S.; Moyano, F.; Falcone, R. D.; Silber, J. J.; Correa, N. M. *J. Phys. Chem. B* **2009**, *113*, 6718–6724.
(20) Moyano, F.; Falcone, R. D.; Mejuto, J. C.; Silber, J. J.; Correa, N. M. *Chem.—Eur. J.* **2010**, *16*, 8887–8893.
(21) Blach, D.; Correa, N. M.; Silber, J. J.; Falcone, R. D *J. Colloid Interface Sci.* **2011**, *355*, 124–130.
(22) García Rios, L.; Godoy, A.; Rodriguez—Dafonte, P. *Eur. J. Org. Chem.* **2006**, 3364–3371.
(23) Abuin, E.; Lissi, E.; Duarte, R.; Silber, J. J.; Biasutti, M. A. *Langmuir* **2002**, *18*, 8340–8344.
(24) Majhi, P. R.; Moulik, S. P. *J. Phys. Chem. B* **1999**, *103*, 5977–5983.
(25) Hait, S. K.; Sanyal, A.; Moulik, S. P. *J. Phys. Chem. B* **2002**, *106*, 12642–12650.
(26) Mukerjee, K.; Moulik, S. P.; Mukherjee, D. P. *Langmuir* **1993**, *9*, 1727–1730.
(27) Ueda, M.; Schelly, Z. A. *J. Colloid Interface Sci.* **1988**, *124*, 673–676.
(28) Heatley, F. *J. Chem. Soc., Faraday Trans* **1988**, *84*, 343–354.
(29) D'Angelo, M.; Fioretto, D.; Onori, G.; Santucci, A. *J. Mol. Struct.* **1996**, *383*, 157–163.
(30) Salabat, A.; Eastoe, J.; Mutch, K. J.; Rico, F.; Tabor *J. Colloid Interface Sci.* **2008**, *318*, 244–251.
(31) Myakonkaya, O.; Eastoe, J.; Mutch, K. J.; Rogers, S.; Heenan, R.; Grillo, I. *Langmuir* **2009**, *25*, 2743–2748.
(32) Hollamby, M. J.; Tabo, R.; Mutch, K. J.; Trickett, K.; Eastoe, J.; Heenan, R. K.; Grillo, I. *Langmuir* **2008**, *24*, 12235–12240.
(33) Hou, M. J.; Kim, M.; Shah, D. O. *J. Colloid Interface Sci.* **1988**, *123*, 398–412 and references in the text.
(34) Cazabat, A. M.; Langevin, D. *J. Chem. Phys.* **1981**, *74*, 3148–3158.
(35) Lemaire, B.; Bothorel, P.; Roux, D. *J. Phys. Chem.* **1983**, *87*, 1023–1028.
(36) Huang, J. S. *J. Chem. Phys.* **1985**, *82*, 480–484.
(37) Calje, A. A.; Agterof, W. G. M.; Vrij, A. In *Micellization, Solubilization and Microemulsions*; Mittal, K. L., Ed.' Plenum: New York, 1977; Vol 2, p 779.
(38) Ueda, M.; Schelly, Z. A. *Langmuir* **1989**, *5*, 1005–1008.
(39) Iloukhani, H.; Sameti, M. R.; Parsa, J. B. *J. Chem. Termodyn.* **2006**, *38*, 975–982.
(40) Dimroth, K.; Reichardt, C.; Siepmann, T.; Bohlmann, F. *Ann. Chem.* **1963**, *661*, 1–37.
(41) Falcone, R. D.; Correa, N. M.; Silber, J. J. *Langmuir* **2009**, *25*, 10426–10429.
(42) Marcus, Y. *Chem. Soc. Rev.* **1993**, *22*, 409–416.
(43) Durantini, A. M.; Falcone, R. D.; Silber, J. J.; Correa, N. M. *J. Phys. Chem. B* **2011**, *115*, 5894–5902.
(44) Reichardt, C. *Solvent and Solvent Effects in Organic Chemistry*, 2nd ed.; VCH: New York, 1990.
(45) Fletcher, P. D. I.; Galal, M. F.; Robinson, B. H. *J. Chem. Soc., Faraday Trans. I* **1984**, *80*, 3307–3314.
(46) Reiter, R. E.; Undiks, E. P.; Kimmel, J. R.; Levinger, N. E. *J. Phys. Chem. B* **1998**, *102*, 7931–7938.
(47) Riter, E. R.; Kimmel, J. R.; Undiks, E. P.; Levinger, N. E. *J. Phys. Chem. B* **1997**, *101*, 8292–8297.
(48) Eastoe, J.; Gold, S.; Rogers, S. E.; Paul, A.; Welton, T.; Heenan, R. K.; Grillo, I. *J. Am. Chem. Soc.* **2005**, *127*, 7302–7303.
(49) Gao, Y.; Li, N.; Zheng, L.; Bai, X.; Yu, L.; Zhao, X.; Zhang, J.; Zhao, M.; Li, Z. *J. Phys. Chem. B* **2007**, *111*, 2506–2513.
(50) Fletcher, P. D. L.; Howe, A. M.; Robinson, B. H. *J. Chem. Soc. Faraday Trans. 1* **1987**, *1*, 985–1006.
(51) Brunetti, S.; Roux, D.; Bellocq, A. M.; Fourche, G.; Bothorel, P. *J. Phys. Chem.* **1983**, *87*, 1028–1034.
(52) Huang, J. S.; Safran, S. A.; Kim, M. W.; Grest, G. S.; Kotlarchyk, M.; Quirke, N. *Phys. Rev. Lett.* **1984**, *53*, 592–595.
(53) (a) Eastoe, J.; Dong, J.; Hetherington, K. J.; Steytler, D. C.; Heenan, R. K. *J. Chem. Soc. Faraday Trans.* **1996**, *92*, 65–72. (b) Eastoe, J.; Hetherington, K. J.; Sharpe, D.; Dong, J.; Heenan, R. K.; Steytler, D. C. *Langmuir* **1996**, *12*, 3876–3880. (c) Eastoe, J.; Hetherington, K. J.; Sharpe, D.; Steytler, D. C.; Egelhaaf, S.; Heenan, R. K. *Langmuir* **1997**, *13*, 2490–2493.
(54) Maitra, A. *J. Phys. Chem.* **1984**, *88*, 5122–5125.
(55) Li, Q.; Li, T.; Wu, J. *J. Colloid Interface Sci.* **2001**, *239*, 522–527.
(56) Evans, D. F.; Ninham, B. W. *J. Phys. Chem.* **1986**, *90*, 226–234.
(57) Falcone, R. D.; Silber, J. J.; Correa, N. M. *Phys. Chem. Chem. Phys.* **2009**, *11*, 11096–11100.